THE JOURNAL OF PHYSICAL CHEMISTRY A

 VOLUME 104, NUMBER 35, SEPTEMBER 7, 2000

ARTICLES

Photodissociation Dynamics of Hydrated Ni^{2+} Clusters: $Ni^{2+}(H_2O)_n$ ($n = 4-7$)

Christopher J. Thompson, John Husband, Fernando Aguirre, and Ricardo B. Metz*

Department of Chemistry, University of Massachusetts-Amherst, Amherst, Massachusetts 01003

Received: April 24, 2000; In Final Form: July 5, 2000

Hydrated divalent nickel clusters, $Ni^{2+}(H_2O)_n$ ($n = 4-7$), have been generated through electrospray ionization and studied with laser photofragment spectroscopy. Clusters containing six and seven water molecules dissociate by loss of either one or two water molecules. In contrast, $Ni^{2+}(H_2O)_4$ dissociates via charge reduction, producing $H_3O^+ + NiOH^+(H_2O)_2$. The modest kinetic energy release in the H_3O^+ product is in agreement with a salt-bridge dissociation mechanism. Observed dissociation cross-sections indicate that the hexahydrated species is the probable carrier for nickel's aqueous absorption spectrum.

Introduction

Solvation of transition metals lies at the heart of much of condensed-phase chemistry and biochemistry. A complete understanding of solvation requires that one look beyond the bulk properties and concentrate on the microscopic environment around the metal ion. One way to do this in a controlled fashion is through gas-phase studies of solvation. However, most of these studies have focused on singly charged metal ions[1−4] rather than the multiply charged species typical of transition metals in solution. In aqueous solution, first-row transition metal dications (M^{2+}) are surrounded by an inner solvation shell of six water molecules resulting in an octahedral, or nearly octahedral, $M^{2+}(H_2O)_6$ species.[5] According to simple crystal field theory, the resulting field splits the degenerate atomic 3d orbitals into a set of e_g and t_{2g} orbitals. Transitions between these orbitals are responsible for the characteristic visible and near-ultraviolet absorption spectra of transition metals. Because d−d transitions are symmetry forbidden in the isolated M^{2+}, transitions between the levels are quite weak, with typical extinction coefficients of $\epsilon = 1-10\ M^{-1}\ cm^{-1}$.[6]

The advent of electrospray ion sources[7] (ESI) has allowed scientists to directly study multiply charged gas-phase clusters that maintain the local solution environment around the metal ion. Several groups have examined transition metal $M^{2+}(H_2O)_n$ systems from both an experimental and a theoretical viewpoint. Kebarle and co-workers measured the equilibrium for the hydration reaction

$$M^{2+}(H_2O)_n + H_2O \leftrightarrows M^{2+}(H_2O)_{n+1} \qquad (1)$$

for the transition metals from Mn to Zn, determining ΔG for the process.[8,9] The experiments were limited to clusters with $n = 8-13$, and assuming $\Delta S = 96$ J/(K mol), led to an outer-shell hydration energy of ~63 kJ/mol. They also performed collision induced dissociation (CID) studies on both inner- and outer-shell species, which showed loss of water as the only channel for large clusters. They observed a competitive charge-reduction channel

$$M^{2+}(H_2O)_n \rightarrow MOH^+(H_2O)_{n-2} + H_3O^+ \qquad (2)$$

for clusters containing fewer than a critical number of water ligands. The number of ligands required for the onset of charge reduction increases with the ionization energy of M^+. More recently, Williams and co-workers[10] used blackbody infrared radiative dissociation (BIRD) to directly measure hydration energies of $Ni^{2+}(H_2O)_n$ ($n = 5-7$), obtaining a bond strength of 100 ± 4 kJ/mol for the sixth water on $Ni^{2+}(H_2O)_6$. Posey and co-workers used photofragment spectroscopy to investigate solvation of ligated transition metal dications such as $Fe^{2+}(bpy)_3$ and $Fe^{2+}(terpy)_2$.[11,12] The effects of both the nature and the

* To whom correspondence should be addressed (E-mail: rbmetz@chemistry.umass.edu).

10.1021/jp001554r CCC: $19.00
Published on Web 08/15/2000

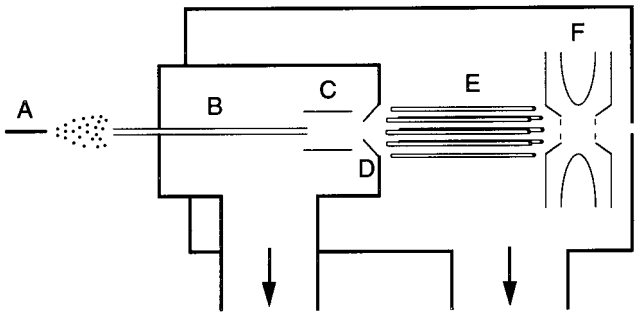

Figure 1. Schematic of the electrospray source. Labels are described in the text.

number of solvent molecules on the strongly allowed ($\epsilon \approx 10\,000$ M^{-1} cm^{-1}) metal-to-ligand charge transfer band were studied. These studies revealed photofragment spectra that are similar to, but slightly shifted from solution absorption spectra, implying that the oxidation state of the metal in solution is retained in the gas phase.

Although there have been many theoretical studies of hydrated divalent *alkaline earth* metals,[13−16] there have been relatively few studies of the corresponding transition metal systems. Åkesson et al.[17] used SCF methods to find the total binding energy of six H_2O molecules to the first-row transition metals, while Åkesson and Pettersson[18] calculated the first and second hydration energies for the same transition metals. Sandström and co-workers[15] used the B3LYP method to find sequential binding energies of the first six H_2O molecules to Zn^{2+}. In addition to thermochemical analysis, theorists have sought to identify the specific carrier in the transition metal aqueous absorption spectra. In the most detailed study, Gilson and Krauss[19] used complete active space-multiconfiguration self-consistent field (CAS-MCSCF) and multiconfigurational quasi-degenerate perturbation theory (MCQDPT) calculations to compute transition energies and oscillator strengths for the tetra-, penta-, and hexahydrate Co^{2+}species. In addition, they computed the spectrum of ions formed by substituting a hydroxide ion for a water molecule in each species. They proposed that the most abundant aqueous species, $Co^{2+}(H_2O)_6$, is not the carrier of aqueous absorption because it has a very low ($<10^{-6}$) oscillator strength. To obtain an oscillator strength of 1×10^{-6}, the axial waters had to be distorted from octahedral symmetry by 0.15 Å. For comparison, if the hexahydrate is assumed to be responsible for cobalt's aqueous absorption peak near 510 nm, conversion of the integrated absorption coefficient[20] yields an approximate oscillator strength of 3.3×10^{-5}. All of the five remaining species are predicted to absorb. They suggest that aqueous absorption is due to the pentahydrate with some contribution from the tetrahydrate at high temperature.[21]

In this work, the absorption properties and photodissociation dynamics of hydrated nickel dications, $Ni^{2+}(H_2O)_n$ ($n = 4-7$), are investigated. The effect of coordination number on the absorption spectrum is examined and dissociation channels are monitored as a function of cluster size.

Experimental Section

Gas-phase $Ni^{2+}(H_2O)_n$ ions are produced using a home-built electrospray ion source and studied in a reflectron time-of-flight (RTOF) mass spectrometer.[22] A schematic of the electrospray source is given in Figure 1. Clusters are formed under atmospheric conditions from a 3.0×10^{-4} M solution of $NiCl_2$ in distilled water, which flows at a rate of 0.3 mL/hr through a 0.11 mm i.d., 0.47 mm o.d. (26s gauge) stainless steel (s.s.) needle (A in Figure 1) held at 7 kV. Ions enter the interface

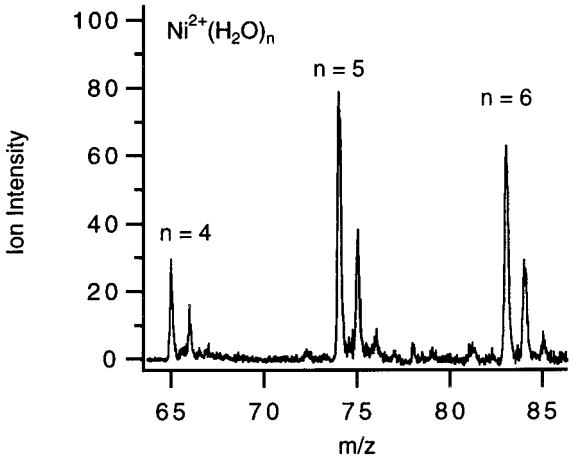

Figure 2. Mass spectrum of hydrated divalent nickel clusters. Clusters containing the two major ^{58}Ni and ^{60}Ni isotopes are separated by one *m*/*z* unit showing their divalent nature. The major ^{58}Ni isotope was used throughout the study.

chamber, which is maintained at ~1 Torr by an 8.3 L/s mechanical pump, through a heated 23 cm long, 0.51 mm i.d., 1.59 mm o.d. s.s. desolvation tube[23] (B) held between 0 and 100 V. The needle−desolvation tube distance and orientation can be adjusted; they are typically collinear and ~1 cm apart. After exiting the desolvation tube, ions are focused with a tube lens (C) and pass through a 1 mm diameter skimmer (D) typically held at 5−30 V, into the source chamber maintained at 3×10^{-4} Torr by a 6 in. diffusion pump. A 10 cm long home-built octopole ion guide[24,25] (E) leads the ions into an rf ion trap (RM Jordan Co., F). The ion trap serves to couple[26,27] the continuous ESI source to an existing pulsed (20 Hz) RTOF instrument that can also be used with a pulsed laser ablation source.[22,28] Ions are trapped for a maximum of 49 ms and thermalized to 300 K by approximately 1700 collisions with ~1 mTorr helium and 600 collisions with ~0.3 mTorr air. Using thermalized ions allows for a better comparison between gas-phase ions and room-temperature solution spectra. The rf field applied to the trap has been modified to run in either a standard continuous mode or in a variable pulsed mode that gates the rf field.[29] Running under pulsed conditions aids in the formation of small clusters ($n \leq 5$). Stored ions are injected into the RTOF mass spectrometer by a 110 V pulse applied to the front plate of the trap. This pulse also functions as the extraction field of the Wiley−MacLaren TOF mass spectrometer. Ions are accelerated to ~1800 V, enter the first differential chamber, held at 3×10^{-6} Torr by a 4 in. diffusion pump, and are re-referenced[30] to ground potential. An Einzel lens and deflectors guide the ions into the detector region which is maintained below 2×10^{-7} Torr by a 240 L/s ion pump. A mass spectrum obtained under conditions that favor small clusters is shown in Figure 2.

Mass-selected clusters are excited at the turning point of the reflectron using the unfocused output of a Nd:YAG-pumped dye laser operating at 20 Hz repetition rate. Most of the species studied have a very small photodissociation cross section, so background interference to the fragment signal needs to be minimized. Upon extraction from the ion trap, a small percentage of ions is excited through collisions with background gas molecules, producing unstable clusters that dissociate in the flight tube. Voltages applied to the reflectron are chosen to separate photofragment ions from these background ions. Parent and fragment ion intensities are determined by their flight times to a 40 mm diameter dual microchannel plate detector. Mass spectra are collected on a 500 MHz digital oscilloscope (Tektronics 524A) and averaged on a PowerMac running a

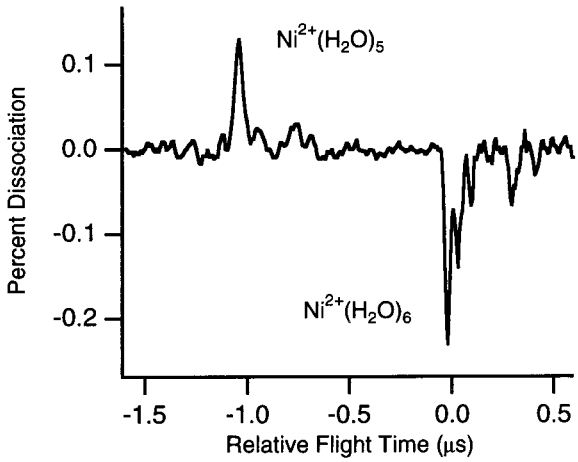

Figure 3. Difference spectrum of $Ni^{2+}(H_2O)_6$ at 735 nm showing loss of H_2O. The small peaks shifted by 0.2 μs from the major peaks are due to photodissociation of the $^{60}Ni^{2+}(H_2O)_6$ isotopomer.

LabView-based program. Fragment channels and branching ratios are determined from *difference spectra* — the difference between spectra obtained with the dissociation laser blocked and unblocked.

Results and Discussion

In aqueous solution, Ni^{2+} has three absorption peaks in the visible and near-UV region: at 395 nm ($\epsilon \approx 5.2\ M^{-1}\ cm^{-1}$) and a doublet in the red with maxima at 658 nm ($\epsilon \approx 1.9\ M^{-1}\ cm^{-1}$) and 725 nm ($\epsilon \approx 2.1\ M^{-1}\ cm^{-1}$).[6] Traditionally, these transitions have been assigned to symmetry-forbidden d−d transitions in the octahedral $M^{2+}(H_2O)_6$ species,[31] with the standard explanation being that the transitions are weakly vibronically allowed.[5,6] However, the ab initio study of Gilson and Krauss[19] on cobalt's absorption properties suggests that a small amount of a strongly absorbing minor species could be responsible for the observed solution spectrum. They identify $M^{2+}(H_2O)_5$ as a likely carrier. This species is formed in solution as the hexahydrate exchanges water ligands.[32,33]

Each of the cluster ions $Ni^{2+}(H_2O)_n$ ($n = 4-7$) is examined in the region of nickel's solution absorption bands. A natural starting point is $Ni^{2+}(H_2O)_6$, the most abundant aqueous species. Because absorption near 725 nm provides 165 kJ/mol of energy, well above the 100 kJ/mol binding energy of the sixth water given by the BIRD experiment,[10] photodissociation provides a useful probe into the absorption properties of the cluster. Figure 3 shows a difference spectrum taken at 735 nm. Photodissociation was investigated from 720 to 840 nm and occurs by the loss of one water molecule. Simple loss of water is consistent with the dissociation channels observed in CID experiments by Kebarle.[8,9] No sharp structure in the photodissociation cross section was observed over the region studied. Two-photon absorption needs to be considered for $Ni^{2+}(H_2O)_6$, because the d−d transitions are symmetry-allowed two-photon transitions and aqueous Ni^{2+} also absorbs near 400 nm. At 815 nm, photodissociation with an unfocused laser beam is linear with laser power (lp) and leads exclusively to loss of one H_2O ligand. Photodissociation using a focused (1 m lens) laser beam is proportional to $(lp)^{1.5}$ and results in loss of H_2O and 2 H_2O. Thus, using an unfocused laser beam leads to one-photon dissociation. The absolute cross section for one-photon photodissociation, estimated by normalizing the percent dissociation to the laser fluence, is 2×10^{-20} cm^2 at 775 nm, which corresponds to an extinction coefficient of $\sim 14\ M^{-1}\ cm^{-1}$. Uncertainties in the absolute cross sections are estimated at 50% and are due to laser beam nonuniformity and uncertainty in the overlap between the laser and ion beams. The $Ni^{2+}(H_2O)_7$ species is in effect the $Ni^{2+}(H_2O)_6$ chromophore with an outer-shell water attached. It also absorbs in this region with a similar cross section to $Ni^{2+}(H_2O)_6$ and dissociates via loss of either one or two water molecules.

Of all the clusters studied, the most surprising result comes from the pentahydrate, for which we observe no photodissociation over the visible and near-UV. Calculations predict that the fifth water molecule is bound to Zn^{2+} by 100 kJ/mol,[15] which corresponds to a threshold of 1190 nm. Because the binding is primarily electrostatic in both Zn^{2+} and Ni^{2+} clusters, photons in the visible should have sufficient energy to photodissociate $Ni^{2+}(H_2O)_5$. Thus, the absence of photodissociation in the region examined is due to limited absorption by the chromophore. We determine an upper limit for the photodissociation cross section $\sigma < 3 \times 10^{-21}$ cm^2 at 355 nm, on the basis of <0.15% fragmentation upon irradiation with 50 mJ/pulse. This result suggests that $Ni^{2+}(H_2O)_5$ is not responsible for the aqueous absorption bands.

The minor $Ni^{2+}(H_2O)_4$ species is expected to absorb more strongly than the hexahydrate, because it has a tetrahedral geometry, which lacks a center of inversion. Generally, tetrahedral complexes have d−d transitions that are 1−2 orders of magnitude more intense than octahedral complexes.[5] Examina-

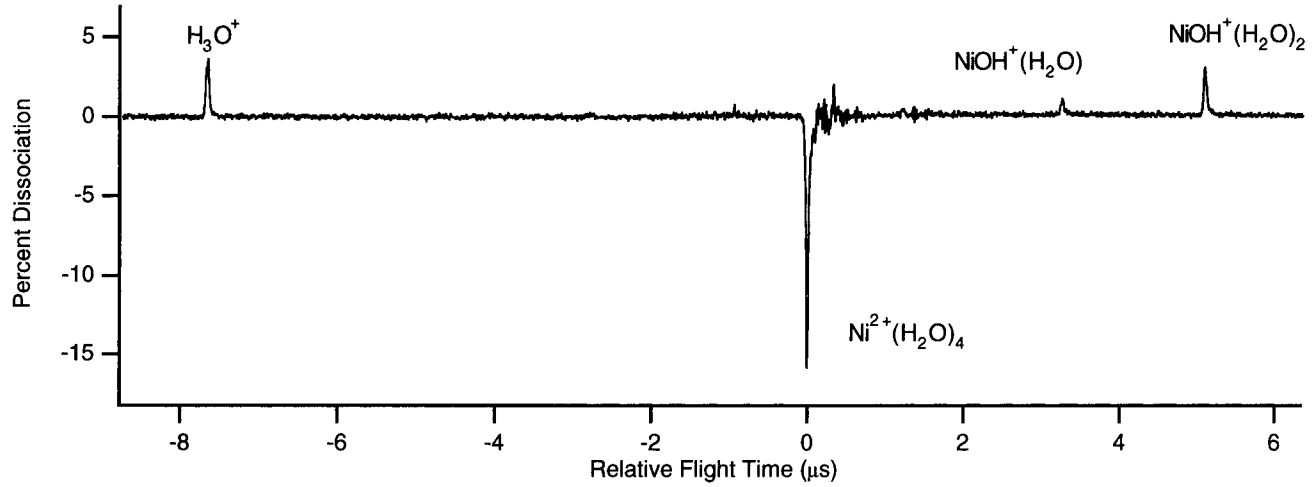

Figure 4. Difference spectrum of $Ni^{2+}(H_2O)_4$ at 570 nm. Primary dissociation is to $NiOH^+(H_2O)_2 + H_3O^+$. Subsequent photodissociation of $NiOH^+(H_2O)_2$ likely produces $NiOH^+(H_2O)$.

tion of the tetrahydrate species as a possible carrier is backed by the observation of absorption assigned to $Co^{2+}(H_2O)_4$ in high-temperature aqueous cobalt solution.[21] We measured the photofragment spectrum of $Ni^{2+}(H_2O)_4$ over the range 490 to 740 nm, observing a broad feature with a maximum cross section of 7×10^{-20} cm^2 ($\epsilon \approx 44$ M^{-1} cm^{-1}) at 570 nm. Comparison to $Ni^{2+}(H_2O)_6$ ($\epsilon \approx 14$ M^{-1} cm^{-1}) shows no dramatic difference in the maximum absorption properties between the two species. This leads to the $Ni^{2+}(H_2O)_6$ complex being assigned as responsible for the aqueous absorption bands, as it is much more abundant than the $Ni^{2+}(H_2O)_4$ complex in aqueous solution at room temperature.

Unlike the hexa- and heptahydrates, which dissociate by simple water loss, $Ni^{2+}(H_2O)_4$ photodissociates via the charge reduction reaction

$$Ni^{2+}(H_2O)_4 + h\nu \rightarrow NiOH^+(H_2O)_2 + H_3O^+ \qquad (3)$$

Neglecting the contribution of the photon, a thermochemical cycle for reaction 3 at 298 K can be written as

$$\Delta H_{\mathrm{rxn}\,3} = \Delta H_{4,0}(Ni^{2+}) - IP(Ni^+) + IP(H_2O) + PA(OH) - PA(H_2O) - D(Ni^+-OH) - D(NiOH^+-H_2O) - D(NiOH^+H_2O-H_2O) \qquad (4)$$

which is an extension of the cycle used by Kebarle.[9] The binding energy of four waters to Ni^{2+} is estimated based on theoretical calculations[15,17] as $\Delta H_{4,0}(Ni^{2+}) = 1200$ kJ/mol. Proton affinities and ionization potentials are taken from standard reference sources.[34,35] The Ni^+-OH bond strength was determined by photodissociation studies in our laboratory as 257 kJ/mol,[36] while $D(NiOH^+-H_2O)$ and $D(NiOH^+H_2O-H_2O)$ were calculated to be 201 and 116 kJ/mol, respectively, using Gaussian 98[37] at the B3LYP level.[36] Evaluation of the cycle shows the charge reduction channel is *exothermic* by 8 kJ/mol in the absence of a photon. The reactants and products are separated by a significant barrier due to the interaction between the attractive $Ni^{2+}(H_2O)_3-H_2O$ potential and the repulsive $NiOH^+(H_2O)_2-H_3O^+$ potential. The presence of this barrier allows for the observation of the thermodynamically unstable $Ni^{2+}(H_2O)_4$ species.

A difference spectrum of $Ni^{2+}(H_2O)_4$ at 570 nm ($h\nu = 210$ kJ/mol) is shown in Figure 4. Note that both of the charged fragments are observed in the photofragment spectrum. Photodissociation is very selective in that

$$Ni^{2+}(H_2O)_4 + h\nu \rightarrow NiOH^+(H_2O) + H_3O^+(H_2O) \qquad (5)$$

is not observed, although it is ~20 kJ/mol more exothermic than reaction 3. The $H_3O^+(H_2O)$ fragment is bound by 130 ± 6 kJ/mol,[38] and thus should be detected if formed from reaction 5. Because $H_3O^+(H_2O)$ is not observed, the small amount of $NiOH^+(H_2O)$ in Figure 4 is due to either unimolecular dissociation of internally excited $NiOH^+(H_2O)_2$ formed in reaction 3 or, more likely, by secondary photodissociation of the strongly absorbing ($\sigma \approx 1 \times 10^{-17}$ cm^2) $NiOH^+(H_2O)_2$. Photodissociation studies of $NiOH^+(H_2O)_n$ will be published separately.[36] Kebarle's CID study of $Ni^{2+}(H_2O)_4$ also exhibited a charge reduction channel (reaction 3), but differs from our result in that simple ligand loss to $Ni^{2+}(H_2O)_3$ was also observed.

If reaction 3 proceeded via a direct proton-transfer transition state (TS), one would expect, due to the Coulombic repulsion between the adjacent fragment ions, most of the available energy to be released in fragment translation. The kinetic energy release (KER) in this process will lead to broadening in the light H_3O^+ peak. Figure 5 shows an enlargement of the H_3O^+ channel in the difference spectrum of $Ni^{2+}(H_2O)_4$ with the dissociation laser polarization parallel to the ion flight path. Spectra taken at perpendicular laser polarization showed no systematic difference. Also shown in Figure 5 is a simulation[39,40] of the H_3O^+ fragment profile for a total KER of 80 kJ/mol (solid line) and 60 and 100 kJ/mol (dashed lines). The simulation includes the spread in parent ion position and velocity and the finite size of the detector (which causes the small dip in the center of the peak). The total KER is thus 80 ± 20 kJ/mol, with an anisotropy of $\beta = 0.0 \pm 0.3$. Photodissociation of a tetrahedral (spherical top) molecule should occur with an anisotropy of zero.[41]

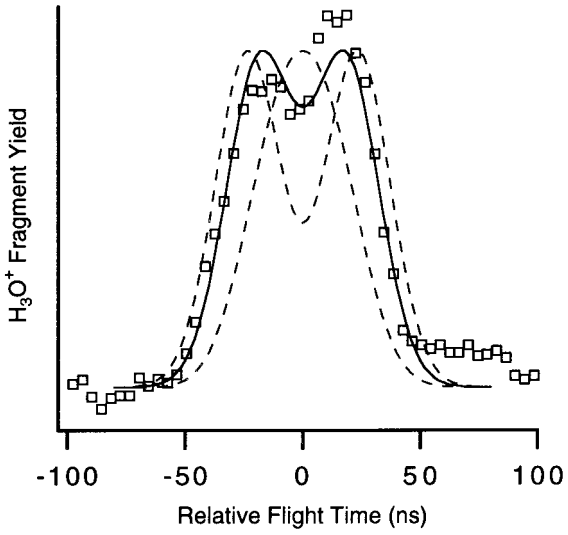

Figure 5. Enlargement of the H_3O^+ channel in the difference spectrum of $Ni^{2+}(H_2O)_4$ taken at 570 nm with the laser polarized parallel to the ion flight path (squares). The solid line is a simulation with a total kinetic energy release (KER) of 80 kJ/mol; simulations at 60 and 100 kJ/mol KER are in dashed lines. All simulations are for an anisotropy $\beta = 0$.

Recently, Bondybey and co-workers[42] used density functional theory to study the charge reduction reaction

$$M^{2+}(H_2O)_2 \rightarrow MOH^+ + H_3O^+ \qquad (6)$$

for the alkaline earth metals M = Be, Mg, Ca, Sr, and Ba. For Mg^{2+} to Ba^{2+} they propose that the reaction takes place through a transition state in which a water molecule moves from the first solvation shell to the second solvation shell before abstracting a proton. At the TS, the complex assumes a salt-bridge arrangement, $M^{2+}-OH^--H_3O^+$, where the oxygen in H_3O^+ is ~6 Å from the metal. The large distance between the positive charges at the TS and the Coulomb attraction between H_3O^+ and the nearby OH^- should lead to relatively low kinetic energy release in the dissociation. Note that a direct inner-shell proton-transfer mechanism should yield a very large KER, because the Coulomb repulsion between two +1 ions is 700 kJ/mol at 2 Å (the inner-shell M − O distance in a typical hydrated M^{2+}) and only decreases to 80 kJ/mol at 17 Å separation.

In a complementary study, Kebarle and co-workers[43] used B3LYP calculations to also examine reaction 6 for $Mg^{2+}$and Ca^{2+}. They find that the TS for charge reduction lies below the TS for simple water loss, but their separation decreases as the number of water ligands is increased. Our observation that photodissociation of $Ni^{2+}(H_2O)_4$ exclusively occurs via charge reduction to form $NiOH^+(H_2O)_2 + H_3O^+$, and that this occurs

with relatively low KER is consistent with a salt-bridge mechanism where one of the four inner-shell waters first moves to the outer shell, then abstracts a proton and departs.

Conclusions

Inner- and outer-shell hydrated nickel dication clusters have been generated through ESI and studied spectroscopically. Although no photofragmentation was observed for the pentahydrate cluster, two distinctive photodissociation pathways are observed in the remaining clusters. $Ni^{2+}(H_2O)_6$ and $Ni^{2+}(H_2O)_7$ dissociate by simply losing either one or two water molecules, whereas $Ni^{2+}(H_2O)_4$ was found to dissociate exclusively through a charge reduction channel to form $NiOH^+(H_2O)_2 + H_3O^+$. A slight anisotropy and only modest kinetic energy release were observed in the H_3O^+ channel. This result is in agreement with recent ab initio calculations that propose a salt-bridge structure for the dissociative transition state in the proton-transfer channel in hydrated alkaline earth dications.

Acknowledgment. Support by the donors of the Petroleum Research Fund, administered by the American Chemical Society, is gratefully acknowledged.

References and Notes

(1) Keese, R. G.; A. W. Castleman, J. *J. Phys. Chem. Ref. Data* **1986**, *15*, 1011−1071.
(2) Duncan, M. A. *Annu. Rev. Phys. Chem.* **1997**, *8*, 69−93.
(3) Eller, K.; Schwarz, H. *Chem. Rev.* **1991**, *91*, 1121−1177.
(4) *Organometallic Ion Chemistry*; Freiser, B. S., Ed.; Kluwer Academic Publishers: Dordrecht, 1996; Vol. 15.
(5) Cotton, F. A.; Wilkinson, G. *Advanced Inorganic Chemistry*, 4th ed.; Wiley-Interscience: New York, 1980.
(6) Sutton, D. *Electronic Spectra of Transition Metal Complexes*, 1st ed.; McGraw-Hill: London, 1968.
(7) Yamashita, M.; Fenn, J. B. *J. Phys. Chem.* **1984**, *88*, 4451−4459.
(8) Blades, A. T.; Jayaweera, P.; Ikonomou, M. G.; Kebarle, P. *J. Chem. Phys.* **1990**, *92*, 5900−5906.
(9) Blades, A. T.; Jayaweera, P.; Ikonomou, M. G.; Kebarle, P. *Int. J. Mass Spectrom.* **1990**, *102*, 251−267.
(10) Rodrigues-Cruz, S. E.; Jockush, R. A.; Williams, E. R. *J. Am. Chem. Soc.* **1998**, *120*, 5842−5843.
(11) Spence, T. G.; Burns, T. D.; Guckenberger, G. B.; Posey, L. A. *J. Phys. Chem. A* **1997**, *101*, 1081−1092.
(12) Spence, T. G.; Trotter, B. T.; Burns, T. D.; Posey, L. A. *J. Phys. Chem. A* **1998**, *102*, 6101−6106.
(13) Katz, A. K.; Glusker, J. P.; Beebe, S. A.; Bock, C. W. *J. Am. Chem. Soc.* **1996**, *118*, 5752−5763.
(14) Glendening, E. D.; Feller, D. *J. Phys. Chem.* **1996**, *100*, 4790−4797.
(15) Pavlov, M.; Siegbahn, P. E. M.; Sandström, M. *J. Phys. Chem. A* **1998**, *102*, 219−228.
(16) Alcamí, M.; González, A. I.; Mó, O.; Yáñez, M. *Chem. Phys. Lett.* **1999**, *307*, 244−252.
(17) Åkesson, R.; Pettersson, L. G. M.; Sandström, M.; Siegbahn, P. E. M.; Wahlgren, U. *J. Phys. Chem.* **1992**, *96*, 10773−10779.
(18) Åkesson, R.; Pettersson, L. G. M. *Chem. Phys.* **1994**, *184*, 85−95.
(19) Gilson, H. S. R.; Krauss, M. *J. Phys. Chem. A* **1998**, *102*, 6525−6532.
(20) Okabe, H. *Photochemistry of Small Molecules*; Wiley-Interscience: New York, 1978.
(21) Swaddle, T. W.; Fabes, L. *Can. J. Chem.* **1980**, *58*, 1418−1426.
(22) Husband, J.; Aguirre, F.; Ferguson, P.; Metz, R. *J. Chem. Phys.* **1999**, *111*, 1433−1437.
(23) Chowdhury, S. K.; Katta, V.; Chait, B. T. *J. Rapid Commun. Mass Spectrom.* **1990**, *4*, 81−87.
(24) Gerlich, D. *Adv. Chem. Phys.* **1992**, *82*, 1−176.
(25) Jones, R. M.; Gerlich, D.; Anderson, S. L. *Rev. Sci. Instrum.* **1997**, *68*, 3357−3362.
(26) Michael, S. M.; Chien, B. M.; Lubman, D. *Anal. Chem.* **1993**, *65*, 2614−2620.
(27) Chien, B. M.; Michael, S. M.; Lubman, D. M. *Int. J. Mass Spectrom.* **1994**, *131*, 149−179.
(28) Aguirre, F.; Husband, J.; Thompson, C. J.; Metz, R. B. *Chem. Phys. Lett.* **2000**, *318*, 466−470.
(29) Quarmby, S. T.; Yost, R. A. *Int. J. Mass Spectrom.* **1999**, *190*, 81−102.
(30) Posey, L. A.; DeLuca, M. J.; Johnson, M. A. *Chem. Phys. Lett.* **1986**, *131*, 170−174.
(31) Holmes, O. G.; McClure, D. S. *J. Chem. Phys.* **1957**, *26*, 1686−1694.
(32) Åkesson, R.; Pettersson, L. G.; Sandström, M.; Siegbahn, P. E.; Wahlgren, U. *J. Phys. Chem.* **1993**, *97*, 3765−3774.
(33) Ducommun, Y.; Newman, K. E.; Merbach, A. E. *Inorg. Chem.* **1980**, *19*(9), 3696−3703.
(34) Hunter, E. P.; Lias, S. G. Proton affinity evaluation In *NIST Chemistry WebBook, NIST Standard Reference Database Number 69*; Mallard, W. G., Linstrom, P. J., Eds.; National Institute of Standards and Technology: Gaithersburg, MD, February 2000. (http://webbook.nist.gov).
(35) *Handbook of Chemistry and Physics*; Weast, R. C., Ed.; CRC Press: Boca Raton, FL, 1985.
(36) Thompson, C. J.; Aguirre, F.; Husband, J.; Metz, R. B. *J. Phys. Chem. A* submitted for publication, 2000.
(37) Frisch, M. J.; Trucks, G. W.; Schlegel, H. B.; Scuseria, G. E.; Robb, M. A.; Cheeseman, J. R.; Zakrzewski, V. G.; Montgomery, J. A.; Stratmann, R. E.; Burant, J. C.; Dapprich, S.; Millam, J. M.; Daniels, A. D.; Kudin, K. N.; Strain, M. C.; Farkas, O.; Tomasi, J.; Barone, V.; Cossi, M.; Cammi, R.; Mennucci, B.; Pomelli, C.; Adamo, C.; Clifford, S.; Ochterski, J.; Petersson, G. A.; Ayala, P. Y.; Cui, Q.; Morokuma, K.; Malick, D. K.; Rabuck, A. D.; Raghavachari, K.; Foresman, J. B.; Cioslowski, J.; Ortiz, J. V.; Stefanov, B. B.; Liu, G.; Liashenko, A.; Piskorz, P.; Komaromi, I.; Gomperts, R.; Martin, R. L.; Fox, D. J.; Keith, T.; Al-Laham, M. A.; Peng, C. Y.; Nanayakkara, A.; Gonzalez, C.; Challacombe, M.; Gill, P. M. W.; Johnson, B. G.; Chen, W.; Wong, M. W.; Andres, J. L.; Head-Gordon, M.; Replogle, E. S.; Pople, J. A. *Gaussian 98*, Revision A.3; Gaussian, Inc.: Pittsburgh, PA, 1998.
(38) Dalleska, N. F.; Homma, K.; Armentrout, P. B. *J. Am. Chem. Soc.* **1993**, *115*, 12125−12131.
(39) Ding, L. N.; Kleiber, P. D.; Young, M. A.; Stwalley, W. C.; Lyyra, A. M. *Phys. Rev. A* **1993**, *48*, 2024−2030.
(40) Cheng, Y. C.; Chen, J.; Klieber, P. D.; Young, M. A. *J. Chem. Phys.* **1997**, *107*, 3758−3765.
(41) Yang, S.-C.; Bersohn, R. *J. Chem. Phys.* **1974**, *61*, 4400−4407.
(42) Beyer, M.; Williams, E. R.; Bondybey, V. E. *J. Am. Chem. Soc.* **1999**, *121*, 1565−1573.
(43) Peschke, M.; Blades, A. T.; Kebarle, P. *Int. J. Mass Spectrom.* **1999**, *185*, 685−699.